Chemistry—Methods

Review
doi.org/10.1002/cmtd.202400036

Chemistry Europe
European Chemical Societies Publishing

www.chemistrymethods.org

Integrating Flow Chemistry With Electrospray Ionization Mass Spectrometry

Quentin Duez*[a]

Flow chemistry is a transformative method that facilitates the exploration of chemical reactivity and enables process automation. In this context of high-throughput experimentation, analysing reaction outputs often constitutes a bottleneck. The direct integration of flow chemistry with electrospray ionization mass spectrometry (ESI-MS) is emerging as a method for the real-time monitoring of reaction mixtures in flow conditions, paving the way for reaction optimization and mechanistic investigations. As shown in selected examples, flow chemistry coupled to ESI-MS facilitates the detection and characterization of reaction intermediates and allows for tracking reaction dynamics under continuously changing conditions. Furthermore, establishing direct feedback between the flow setup and the analytical instrument enables the autonomous optimization of experimental conditions based on the real-time MS readout. Altogether, MS approaches hold the potential to streamline the development of complex synthetic pathways in flow.

Introduction

Flow chemistry has become an alternative to traditional batch processes for chemical transformations, especially because it enables to precisely control reaction conditions, thereby improving reproducibility and scalability.[1] The intrinsic modularity of flow chemistry setups facilitates multistep flow synthesis[2] and allows for the handling of heterogenous,[3] photochemical,[4] or electrochemical transformations.[5] It also provides opportunities for optimizing reaction conditions and automating chemical processes, as demonstrated by the growing development of self-driving laboratories capable to autonomously design and optimize reaction conditions for synthesizing novel compounds.[6–8]

With the development of high-throughput experimentation arises the need for analytical solutions to efficiently characterize reaction outputs.[9] Among the commonly available techniques, electrospray ionization mass spectrometry (ESI-MS) stands out as particularly valuable. ESI-MS overcomes the issues typically associated with the analysis of crude reaction mixtures because it enables the detection of individual compounds based on their mass-to-charge (*m/z*) ratios, even if they might be present with low abundance in solution.[10] The sensitivity and rapidity of ESI-MS analyses, along with the capability to gently transfer elusive species to the gas-phase, make it an ideal technique for online reaction monitoring and for the detection of reaction intermediates.[11,12] To move beyond the simple mass detection, ESI-MS can also be coupled with a variety of add-on methods, such as tandem mass spectrometry, ion mobility spectrometry or ion spectroscopy.

The integration of flow reactors with ESI-MS is emerging as a method for capturing detailed snapshots of a reaction medium under well-defined settings. The residence time in the reactor is typically controlled by the total flowrate and reactor volume, while the reaction conditions are determined by the individual inflows of reagents (Figure 1A). By directly connecting the reactor outlet to the ESI source, the reaction outflow can be continuously monitored. Depending on the reaction concentration, the reactor outflow can also be diluted prior to the infusion in the mass spectrometer[13] or sampled through a six-port valve to minimize instrument contamination.[14] Variations in reaction composition are then monitored in real-time by ESI-MS,[15] with the caveat that ion intensities in the mass spectrum do not always correlate with solution concentrations. Indeed, the processes associated to ESI can make it difficult to correlate solution chemistry with mass spectrometry observations. For example, matrix effects arising from the analysis of crude reaction mixtures may influence the ionization efficiency of compounds of interest, leading to ion suppression.[12] Additionally, the concentration changes during ESI can accelerate reactions, or create artifacts irrelevant for solution chemistry.[16,17] Notwithstanding these possible complications, ESI-MS remains a powerful tool for reaction monitoring and mechanistic investigations as demonstrated by recent examples.[18–20] Furthermore, quantitative MS approaches described below have been proposed to address these limitations.

This review article provides a non-exhaustive overview of applications for coupling flow chemistry with ESI-MS. These applications range from the detection of reactive intermediates under fixed conditions to the monitoring of product compositions under continuously changing conditions. As shown in selected examples, the high information density contained in MS data make it a powerful tool to model complex reaction

[a] *Organic Synthesis and Mass Spectrometry Laboratory, University of Mons (UMONS), Mons, Belgium*

***Correspondence:** Quentin Duez, Organic Synthesis and Mass Spectrometry Laboratory, University of Mons (UMONS), Place du Parc 23, 7000 Mons, Belgium.*
Email: quentin.duez@umons.ac.be

systems or optimize experimental conditions towards a defined objective.

Capturing and Characterizing Elusive Intermediates

The sensitivity of ESI-MS allows for the detection of transient species, such as reactive intermediates, even though they might be present with relatively low abundance in solution. However, characterizing highly reactive intermediates beyond simple mass detection is challenging in batch conditions as the targeted species might degrade or rapidly react with other compounds in solution. Preparing the intermediates in a flow reactor with fixed conditions makes it possible to continuously monitor them by ESI-MS after short reaction times (~ ms/s), thus facilitating their analysis by add-on methods (Figure 1A).

Santos and Metzger employed a continuous flow approach to investigate the mechanism of the Ziegler-Natta polymerization of ethene, catalysed by a zirconocene complex Cp_2ZrCl_2 activated by methyl aluminoxane (MAO) (Figure 1B). In this reaction, the catalytically active species $[Cp_2ZrCH_3]^+$ forms a π-complex with ethene, which yields the insertion product. Rapid insertions of ethene lead to the growth of the polymer chain.[21] To capture the very first stages of the polymerization reaction, the reaction between the activated catalyst and ethene can be monitored after a short reaction time (~1.7 s) by coupling a flow reactor with ESI-MS. As shown in Figure 1C, intermediates bearing up to 30 ethene units are already formed within this timeframe. Upon mass selection and reaction with ethene in the gas phase, the intermediate $[Cp_2ZrCH_2CH_2CH_3]^+$ (*m/z* 263) was found to add several ethene molecules, thereby confirming the proposed mechanism.

As mentioned above, the preparation of transient intermediates in flow reactors enables to further probe their structure by add-on techniques, such as ion mobility spectrometry (IMS). IMS separates ions in the gas phase according to their size and shape, making it an ideal technique for resolving isomeric species when coupled with mass spectrometry.[22–24] Roithová, Nolte and coworkers have recently shown that ion mobility-mass spectrometry could resolve isomeric adducts involving porphyrin cage complexes and various ligands.[25] These catalytically active species consist of a glycoluril pocket capped by a porphyrin roof (Figure 2A),[26,27] allowing for the formation of two isomeric host-guest complexes where the metal-bound guest is oriented either inwards or outwards the cavity.[26,28] To investigate the presence of isomeric intermediates during catalytic reactions, they prepared manganese(V)-oxo complexes in a flow reactor by oxidation of a manganese-(III)-porphyrin cage complex with iodosylbenzene (PhIO), and subjected the resulting species to IMS separation. Several isomers were detected for $[MnC(O)]^+$ ions, corresponding to reactive manganese(V)-oxo species with the oxo ligand pointing inside or outside the cage complex ($[M_{in}]^+$ and $[M_{out}]^+$ in Figure 2B). Functionalizing the sidewalls with methyl groups (**Mn*** complexes) was found to hinder the generation of oxo species inside the cavity. The proportions of oxo-ligands inside or outside the cage complexes could be directly correlated with the preferential binding site of the oxidant molecule, thereby providing direct insights into the mechanisms of alkene epoxidation in solution.[29]

Preparing reactive intermediates in a flow reactor also enables to track their speciation and reactivity in solution. For instance, Rodríguez et al. demonstrated the reactivity of iron-acyl-nitrenoid complexes (Figure 3A – species (**2**)) using a three-syringe pump setup (Figure 3B).[30] The nitrenoid complexes were generated *in situ* by mixing a $(TPA)Fe(OTf)_2$ complex (TPA = tris-(2-pyridylmethyl)amine, OTf = triflate) with dioxazolone (**A**). The nitrenoid intermediates are reactive for hydrogen atom transfer (HAT) with thiophenol (PhSH), as evidenced by the detection of $[(TPA)Fe(PhSNHCOPh)]^{2+}$ ions (**4** – Figure 3C). Monitoring the appearance of these species after reaction with PhSH or deuterated PhSD featured a kinetic isotope effect suggesting HAT as the rate-determining step.[30]

In another implementation, Tripodi et al. tracked the generation, speciation, and reactivity of iron(IV)-oxo complexes in a capillary flow reactor (Figure 4A).[31] In their setup, flowrates were controlled by using overpressure in three vials containing respectively an iron(II) complex $(TPA)Fe(OTf)_2$, an oxidant (1-(tert-butylsulfonyl)-2-iodosylbenzene, ArIO) and a substrate (1-methylcyclohexene, che, Figure 4B). This approach allows for cooling the vials containing the individual starting materials, thus preventing the decomposition of highly reactive intermediates. Upon oxidation with ArIO, the generation of iron(IV)-oxo species is observed (Figure 4C). Monitoring the depletion of iron(IV)-oxo complexes with various labile *cis*-ligands upon reaction with che (Figure 4D) revealed that the complex bearing ArIO as *cis*-ligand, which was not considered active in HAT reactions, is the most reactive.

The structure of mass-selected ions in the gas phase, and especially reactive intermediates, is best characterized by spectroscopic techniques such as infrared photodissociation (IRPD) spectroscopy.[32] However, the experimental time required to record a full spectrum makes the study of short-lived intermediates difficult when reactions are carried out in batch.[33] Interfacing flow reactors, where short-lived species are continuously prepared under controlled conditions, and IRPD has enabled the measurements of IR spectra for intermediates

Quentin Duez obtained his PhD in Chemistry in 2020 from the University of Mons (Belgium) in the groups of Profs. Pascal Gerbaux and Jérôme Cornil, focusing on conformational analyses of gaseous (co)polymer ions by mass spectrometry (MS). He then joined the group of Prof. Jana Roithová at Radboud University (The Netherlands) as a postdoctoral researcher to investigate the mechanisms of organic and metal-organic reactions. He later moved to the group of Prof. Wilhelm Huck to develop MS approaches for the analysis of chemical reaction networks. Since 2023, he holds a FNRS postdoctoral fellowship at the University of Mons.

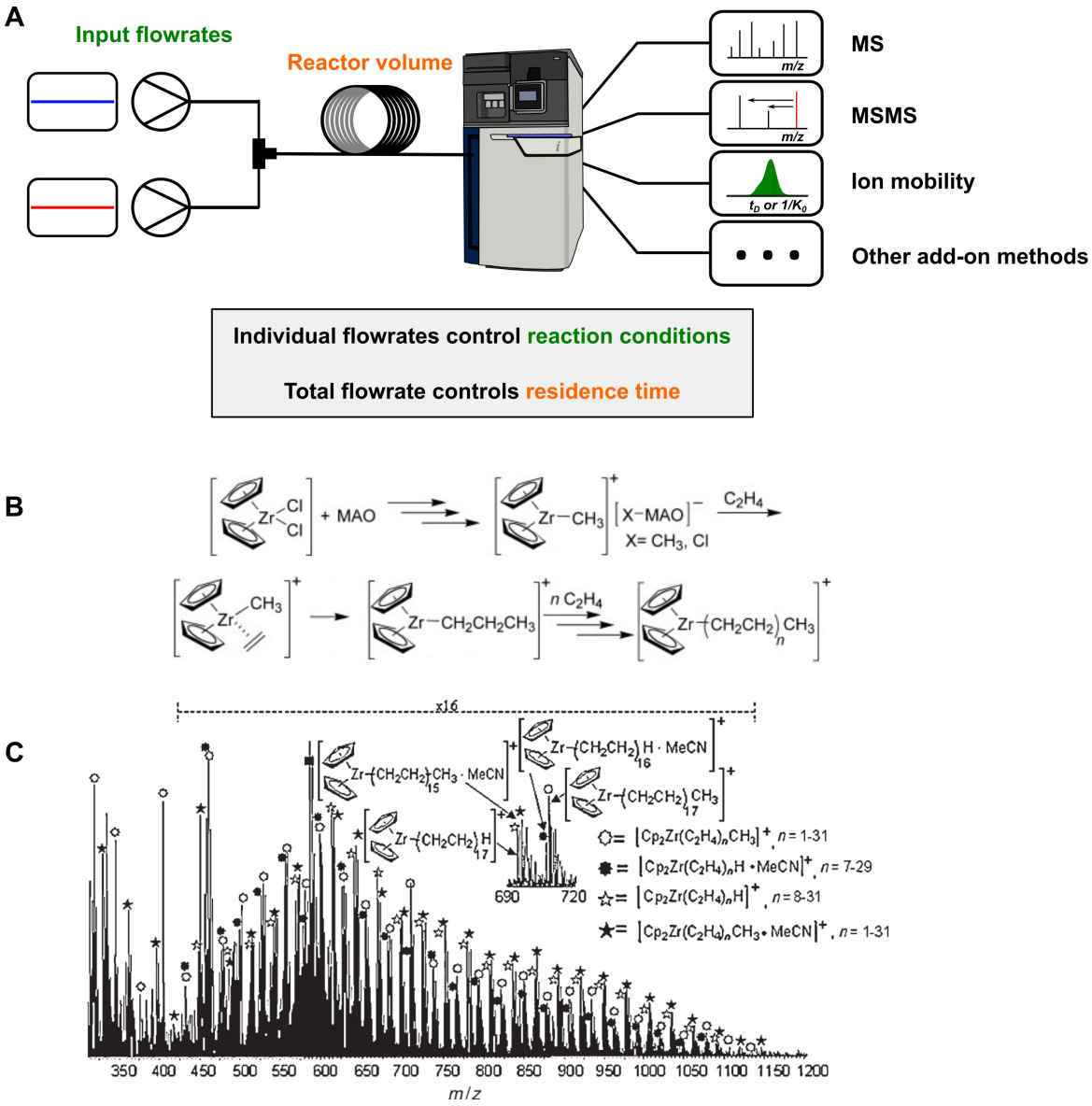

Figure 1. A. Two pumps, containing reagents, dispensing constant flowrates into a flow reactor coupled with a mass spectrometer. B. Proposed mechanism for the Ziegler-Natta polymerization of C_2H_4 catalyzed by Cp_2ZrCl_2/methyl aluminoxane (MAO). C. ESI-MS analysis of the reaction between the preformed (Cp_2ZrCl_2/MAO) catalyst and ethene, after 1.7 s of reaction time. Adapted with permission from reference [21].

in various organic,[33–36] or metal-organic reactions.[31,37,38] In the above example from Tripodi et al. (Figure 4), the reactivity trends correlated well with the stretching frequency of the Fe–O bond measured by IRPD for the iron(IV)-oxo intermediates, thereby providing direct insights into the influence of *cis*-ligands on the reaction in solution.[31] Overall, preparing reactive intermediates in continuous flow conditions is an attractive approach for detection transient species using ESI-MS and complementary methods. This approach opens the way for the characterization of the structure of mass-selected ions in the gas phase, but also for probing their reactivity both in solution and in the gas phase.

Tracking Reaction Dynamics Under Changing Conditions

The swiftness of operation of most ESI-MS instruments allows for the real-time monitoring of reactions in solution with subsecond time resolution.[20,39,40] However, monitoring reaction dynamics in batch conditions is often inadequate to investigate processes taking place within seconds. Moreover, exploring the impact of reaction conditions in batch requires repeating experiments with different initial conditions and piecing together individual results. In contrast, performing chemical transformations in flow enables to rapidly screen through different reaction conditions, while continuously measuring the reaction outcome. Therefore, interfacing flow reactors and ESI-MS opens the way for a real-time readout of how a reaction

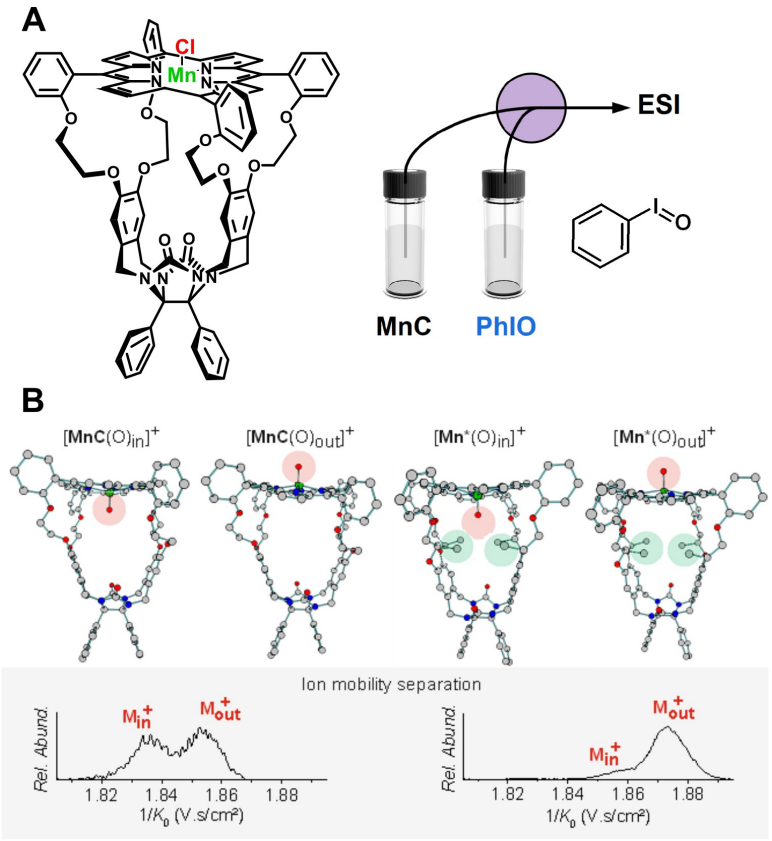

Figure 2. A. Structure of the Mn(III) porphyrin cage complex, and representation of the generation of Mn(V)-oxo complexes in a flow reactor. B. Optimized geometries of $[Mn^{V}C(O)]^{+}$ and the corresponding functionalized species, $[Mn^{V}C^{*}(O)]^{+}$ with the oxo ligand coordinated inside (in) or outside (out) of the cavity, along with the ion mobility separation of mass-selected $[Mn^{V}C(O)]^{+}$ (left) and $[Mn^{V}C^{*}(O)]^{+}$ (right). Adapted with permission from reference [29].

medium adapts to changing conditions, such as adjustments of reagent concentrations, stoichiometry or residence times.

The residence time in a flow reactor is controlled by the reactor size and by the total flowrate. Adjusting either of these parameters provides direct insights on how time influences the reaction outcome. For instance, Jiang et al. modulated the total inflow into a reactor coupled with ESI-MS to monitor the formation of pseudo-rotaxanes in a time-resolved manner.[42] At short reaction times (~ s), they detected wrongly assembled complexes that diverge from the thermodynamically favoured products observed after several minutes or hours. However, changing the total inflow to the ESI source can artificially modulate ion intensities and create ESI artifacts, potentially complicating data interpretation. Konermann et al. addressed this issue by using several reaction capillaries of different lengths while maintaining the overall flowrate constant (Figure 5A), allowing them to monitor protein folding and denaturation with ESI-MS in a time-resolved fashion.[41,43]

As shown in Figure 5B, they could monitor the acid-induced denaturation of holo-myoglobin (hMb) after a pH jump from 6.5 to 3.2 by mixing myoglobin with acetic acid in a reaction capillary. The length of the reaction capillary was varied from 0.9 to 186 cm while keeping the inner diameter fixed, thus providing flow reactors with different volumes. Swapping between different reactors enabled recording a time course of myoglobin denaturation showing two distinct processes. The native hMb unfolds first, which weakens the heme-protein interactions and leads to the detection of hMb20. In the second process, the heme dissociates from the protein, thus yielding apo-myoglobin (aMb).[41] Similarly, Tripodi and colleagues examined the impact of reaction time on the formation and speciation of iron(IV)oxo complexes, and on their subsequent reactivity for oxygen atom transfer reactions using capillary reactors of different lengths.[44]

Although these methods are effective, they involve repeating multiple measurements using different reactors, which constitutes a tedious endeavour. An elegant alternative was proposed by Konermann and Wilson who developed an adjustable reactor with a volume controlled by a stepper motor, enabling to continuously modify the average residence time while monitoring the reaction outcome by ESI-MS.[45] Within a single experiment, they monitored the kinetics of protein demetallation and enzymatic hydrolysis, taking place in less than a second.[46] As shown by the above examples, coupling flow chemistry with ESI-MS enables to efficiently record time-course measurements for fast processes.

The development of automated syringe pumps also enables to rapidly screen various reactions conditions within a single experiment by continuously varying the individual inflows of starting materials to the reactor. For instance, continuously

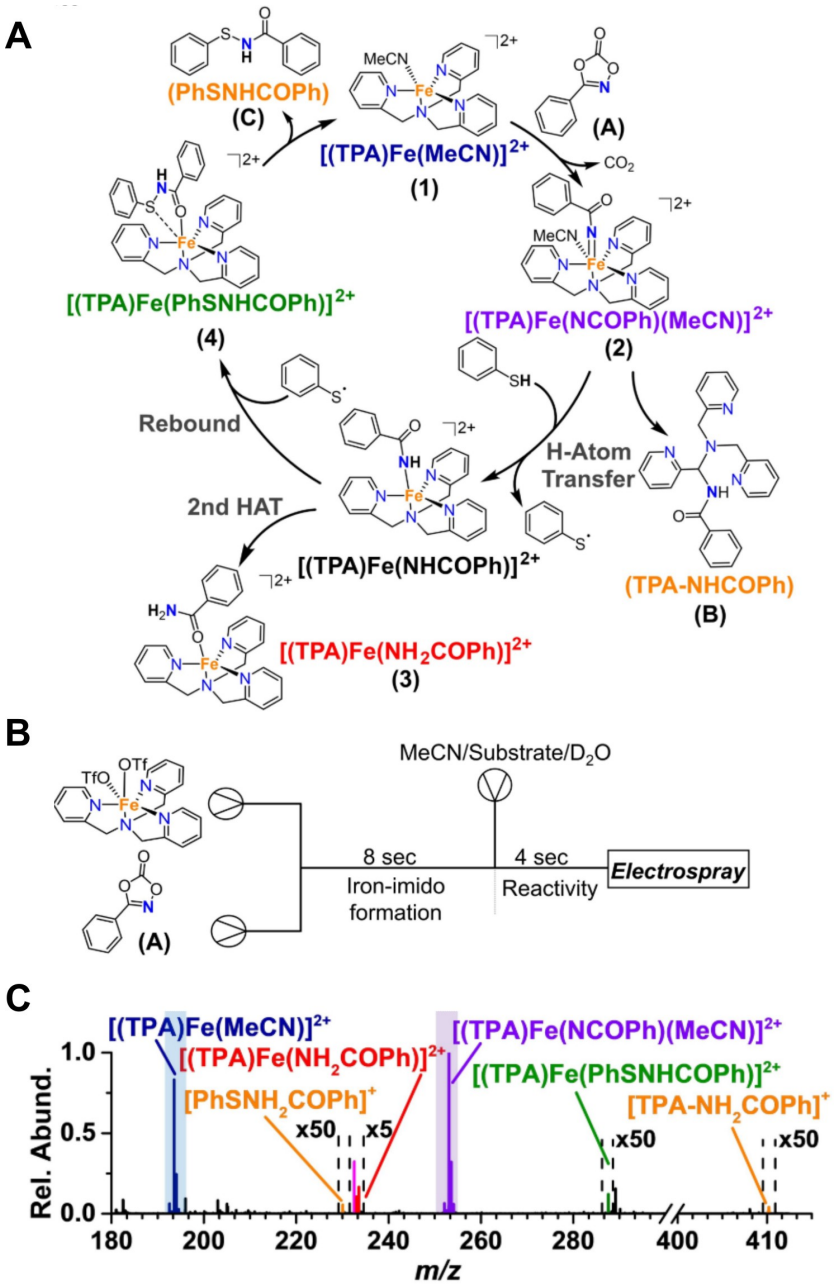

Figure 3. A. Proposed mechanism for iron-acyl-nitrenoid intermediate formation and reactivity with thiophenol (PhSH). B. Flow reactor in which the nitrenoid intermediates are first generated by reaction between (TPA)Fe(OTf)$_2$ and dioxazolone, and subsequently react with PhSH. C. ESI-MS analysis of iron-acyl-nitrenoid intermediates and products from PhSH reaction. Adapted with permission from reference [30].

ramping up the inflow of one reagent enables to assess the impact of its concentration on the reaction outcome (Figure 6A). To vary a single parameter at a time, the reaction time can be kept constant by synchronously decreasing the inflow from another syringe pump containing solvent. Meeus, Derks et al. employed this strategy to investigate the reactivity of nitrene radical complexes with water, aiming to demonstrate that such complexes undergo hydrolysis in water.[47] They formed the nitrene radical cobalt complexes $[Co(TAML)(N^{\bullet}Ts)_n]^-$ (TAML = tetra-amidomacrocyclic ligand ; n = 1, 2) in a flow reactor by reacting a Co(TAML) complex with PhINTs, a nitrene precursor. The reactive species were then subjected to reaction with D_2O in a second reactor. By steadily increasing the flow rate of the syringe containing D_2O while decreasing the flow rate of a make-up syringe containing solvent, they probed the effect of D_2O concentration while maintaining a constant residence time (Figure 6B–C).

As shown by the yellow and light blue traces in Figure 6D, the reaction between the nitrene radical complexes and D_2O leads to the formation of mono- and bis-oxo/oxyl radical species $[Co(TAML)(NTs)(O)]^-$ and $[Co(TAML)(O)_2]^-$ as detected by ESI-MS. The observed species can either be assigned to

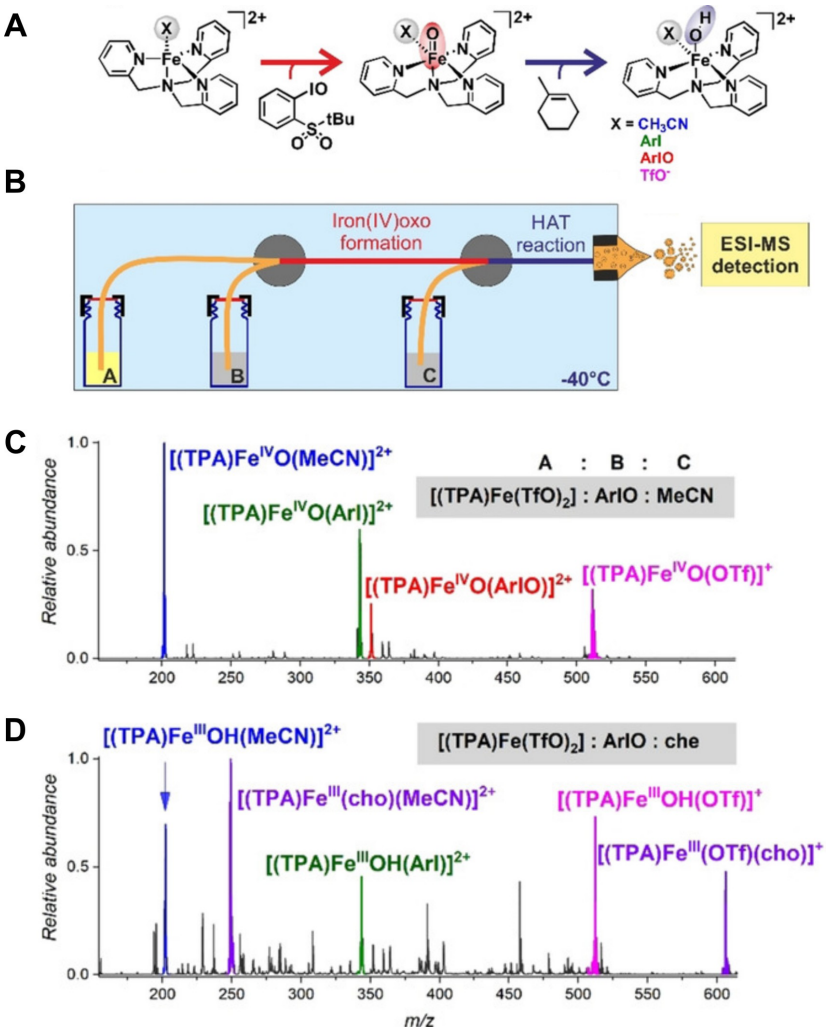

Figure 4. A. Proposed mechanism for iron(IV)-oxo complexes formation by reacting (TPA)Fe(OTf)$_2$ and 1-(tert-butylsulfonyl)-2-iodosylbenzene (ArIO), and subsequent hydrogen atom transfer (HAT) reaction with 1-methylcyclohexene (che). B. Schematic representation of two consecutive flow reactors mixing three reagents (A, B, C), where flowrates are determined by an overpressure in the vials. C and D: ESI-MS analysis of iron(IV)-oxo complexes formation (C contains acetonitrile), and for HAT reactivity (C contains che). Adapted with permission from reference [31].

cobalt-oxo/oxyl radical complexes or to self-oxidized complexes resulting from inter- or intramolecular ligand oxidation at methyl groups of the TAML ligand. Since self-oxidized complexes bear hydroxyl functions, they are expected to undergo rapid H/D exchange in the presence of D_2O. The two dark blue curves show that complexes resulting from H/D exchange grow with increasing D_2O concentration, suggesting that that [Co(TAML)$(O)_2]^-$ converts to another complex containing hydroxyl groups. These results indicate the formation of oxo/oxyl radical species upon hydrolysis of the nitrene radical complexes, which are unstable and undergo inter- or intramolecular oxidation.[47]

Roithová and colleagues used a similar ramping approach to track the formation of intermediates in the Eschenmoser coupling reaction.[36] This reaction yields β-enaminocarbonyl compounds and is proposed to proceed via the formation of thioiminium and thiirane intermediates (S^{1A} and S^{1B} respectively – Figure 7A). The ESI-MS monitoring of this reaction in batch conditions revealed the formation of the expected product and intermediates S^{1A} and S^{1B}, along with polysulfide species containing more sulfur atoms (S^n, with n the number of sulfur atoms) which were never observed before. They noticed that the formation of the intermediates was strongly correlated with initial reagent concentrations. To explore this effect, they designed an experiment to track the evolution of the reaction while continuously increasing the reactant concentration. In this setup, the flow rates of two syringe pumps containing each of the reagents were programmed to increase continuously. To maintain the reaction time constant, the increase in flowrate was counterbalanced by decreasing the inflows of two syringes filled with solvent. The reaction mixture was then diluted with acetonitrile prior to infusion in the ESI-MS instrument (Figure 7B).

As shown in Figure 7C, the polysufide intermediates (S^2 to S^6) appear sequentially with growing reactant concentration, suggesting that their formation involves the consecutive addition of sulfur atoms. Moreover, the appearance of the reaction product is directly correlated with the presence of the S^2 compounds, indicating that the polysulfide species are the

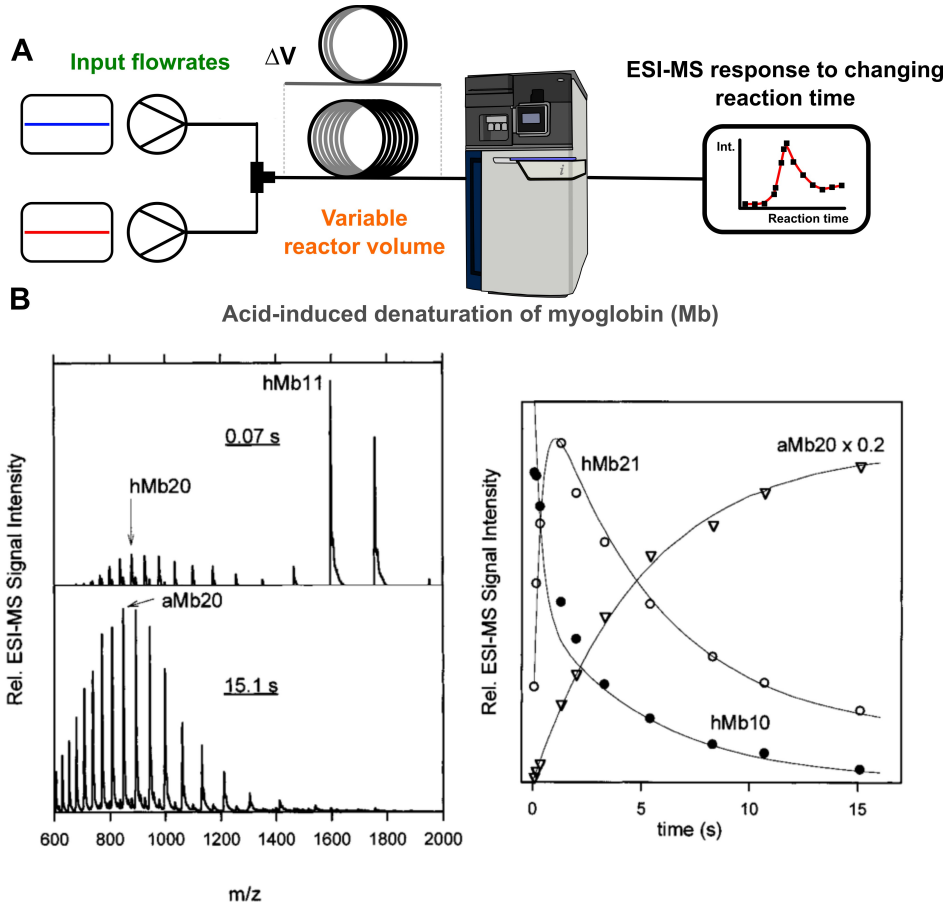

Figure 5. A. Two syringe pumps, containing reagents, dispensing constant flowrates into a flow reactor coupled with a mass spectrometer. By varying the volume of the reactor, the reaction time can be changed without affecting ESI conditions. The measured ESI-MS response corresponds to changes in reaction dynamics depending on the residence time in the reactor. B. Left: ESI-MS spectra of myoglobin (Mb) at 0.07 s and 15.1 s after a pH jump from 6.5 to 3.2. The highlighted ions correspond to hMb11 = [holo-Mb + 11 H]$^{11+}$, hMb20 = [holo-Mb + 20 H]$^{20+}$ and aMb20 = [apo-Mb + 20 H]$^{20+}$. Right: Time course of the three ions highlighted in the left panel. Adapted with permission from reference [41].

key species driving product formation (Figure 7A).[36] Other ramping experiments were also reported to screen the impact of oxidant concentration on the speciation of non-heme iron complexes,[37] or to evaluate the effect of solvent on the degradation of cobalt complexes.[48]

Coupling flow chemistry and ESI-MS can also provide insights into the dynamics of larger reaction networks,[49] such as enzymatic reaction networks (ERN), under changing conditions.[50,51] The underlying kinetics of increasingly complex reaction networks are often poorly understood, which makes them difficult to control and optimize towards a desired outcome.[52] ESI-MS allows for the individual detection of intermediates and products, providing highly informative datasets for modelling network kinetics based on how the system adapts to continuously changing conditions. For instance, Hold and coworkers tracked the metabolic flux of a 10-enzyme cascade producing dihydroxyacetone phosphate (DHAP) from glucose using ESI-MS.[51] The enzymatic reactions took place in a continuous stirred tank reactor (CSTR) to which metabolites were continuously fed by an HPLC pump and in which enzymes or substrates can be added with a HPLC injector (Figure 8). Metabolite quantification was carried out through calibration curves with orthogonal standards, or by using isotopically labelled analytical standards. Because isotopologues share the same ionization efficiency,[25] their relative intensities in a mass spectrum directly relates to their relative concentrations in solution, thus enabling absolute quantification. By breaking down the ERN into subsystems of up to four enzymes, they parametrized a kinetic model by tracking network dynamics through a series of systematic perturbations involving sequential pulses of enzymes or substrates. As shown in Figure 8C, injecting enzymes or pulsing substrates in the CSTR via an HPLC injector causes concentration changes for all substrates, which are continuously monitored by ESI-MS. Simulating these concentration profiles enables to derive kinetic parameters for the enzymatic reactions at play, which in turn allows for optimizing the reaction cascade towards specific outcomes such as improving product yield or minimizing cofactor consumption.[51]

Huck and coworkers later demonstrated that it is possible to gain control over an entire ERN after a single ESI-MS experiment.[53] They immobilized 12 glycolytic enzymes on hydrogel beads and confined them in a CSTR to monitor the response of the entire network to continuously changing

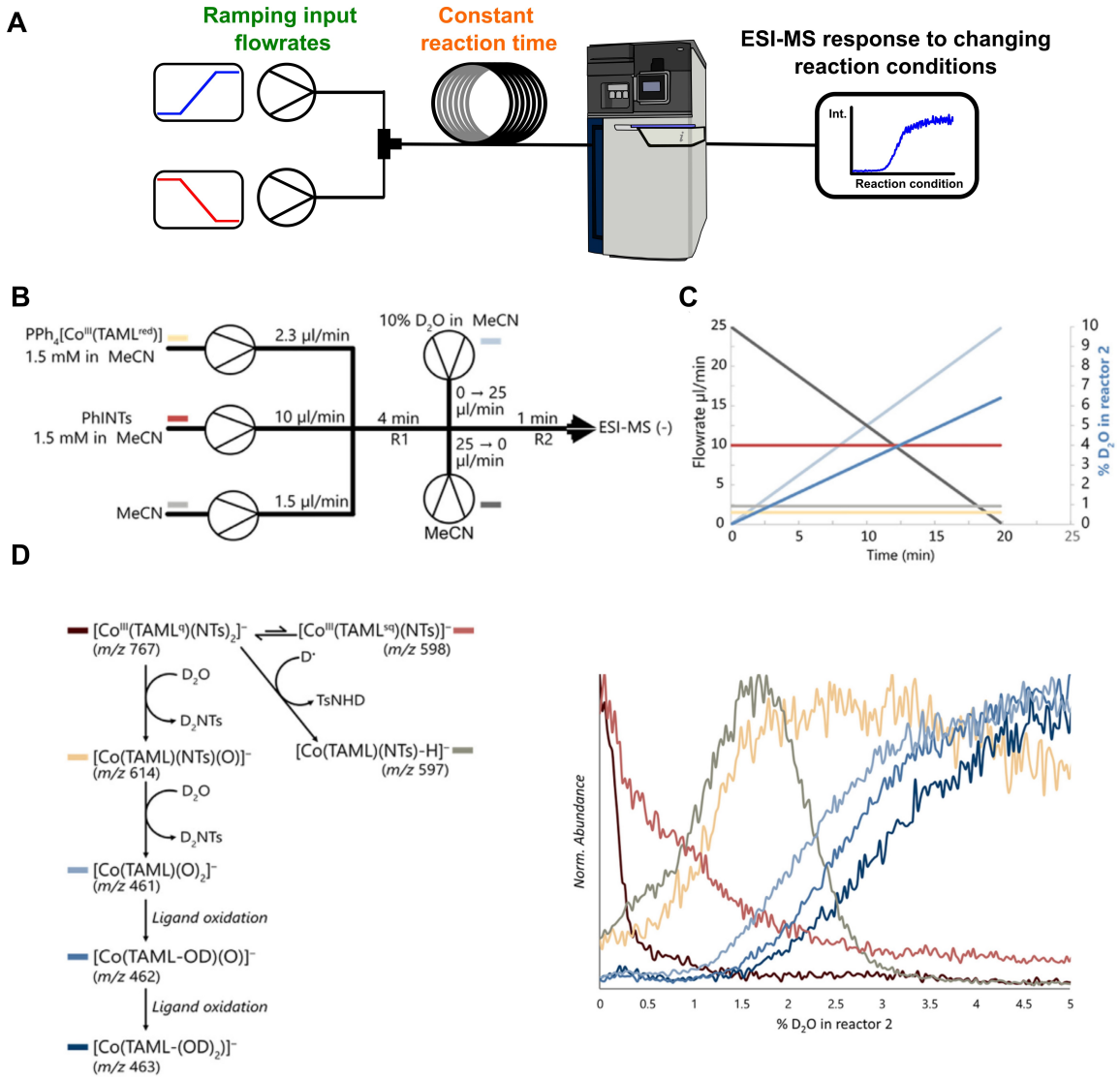

Figure 6. A. Two syringe pumps, containing reagents, dispensing with continuously increasing or decreasing input flowrates into a flow reactor coupled with a mass spectrometer. The measured ESI-MS response corresponds to changes in reaction dynamics according to the changing reaction condition (reagent concentration, stoichiometry, …). B. Flow setup used to investigate the formation of cobalt nitrene radical complexes and subsequent reactivity with D_2O. In this experiment, the flowrate of the syringe containing D_2O is continuously ramped up and counterbalanced by the flowrate of a syringe containing solvent. C. Corresponding flow profile. The blue line shows the $\%D_2O$ in the reactor 2. D. Normalized ESI-MS intensities of the detected complexes with increasing D_2O concentrations. Adapted with permission from reference [47].

conditions. To avoid using isotopically labelled analytical standards, which may be costly or difficult to obtain, they instead generated all isotopically ^{13}C-labelled intermediates and products *in situ* by feeding a uniformly ^{13}C-labelled substrate to the reactor. Diluting the outflow of the reactor with commercially available unlabelled standards then enabled to continuously and quantitatively monitor the metabolic flux of the enzymatic network. Following an optimal experimental design approach,[54] they could train a model of network kinetics after a single optimally designed experiment, thus drastically simplifying the procedure to gain control over ERNs and highlighting the importance of highly informative online monitoring approaches.[53]

Optimizing Experimental Conditions

The design and development of synthetic pathways using conventional batch conditions can be challenging as it often requires numerous experiments with varying experimental conditions to identify the best suited substrates and reaction parameters. Additionally, the efforts needed to monitor reactions and isolate the desired products can hinder progress. Utilizing flow reactors coupled with an online analytical technique such as ESI-MS can tackle this challenge and streamline the screening and optimization of reaction conditions. Indeed, it facilitates the systematic exploration of large input spaces and experimental parameters while continuously monitoring the formation of the desired product, or eventual byproducts. Improvements in yield are typically estimated from

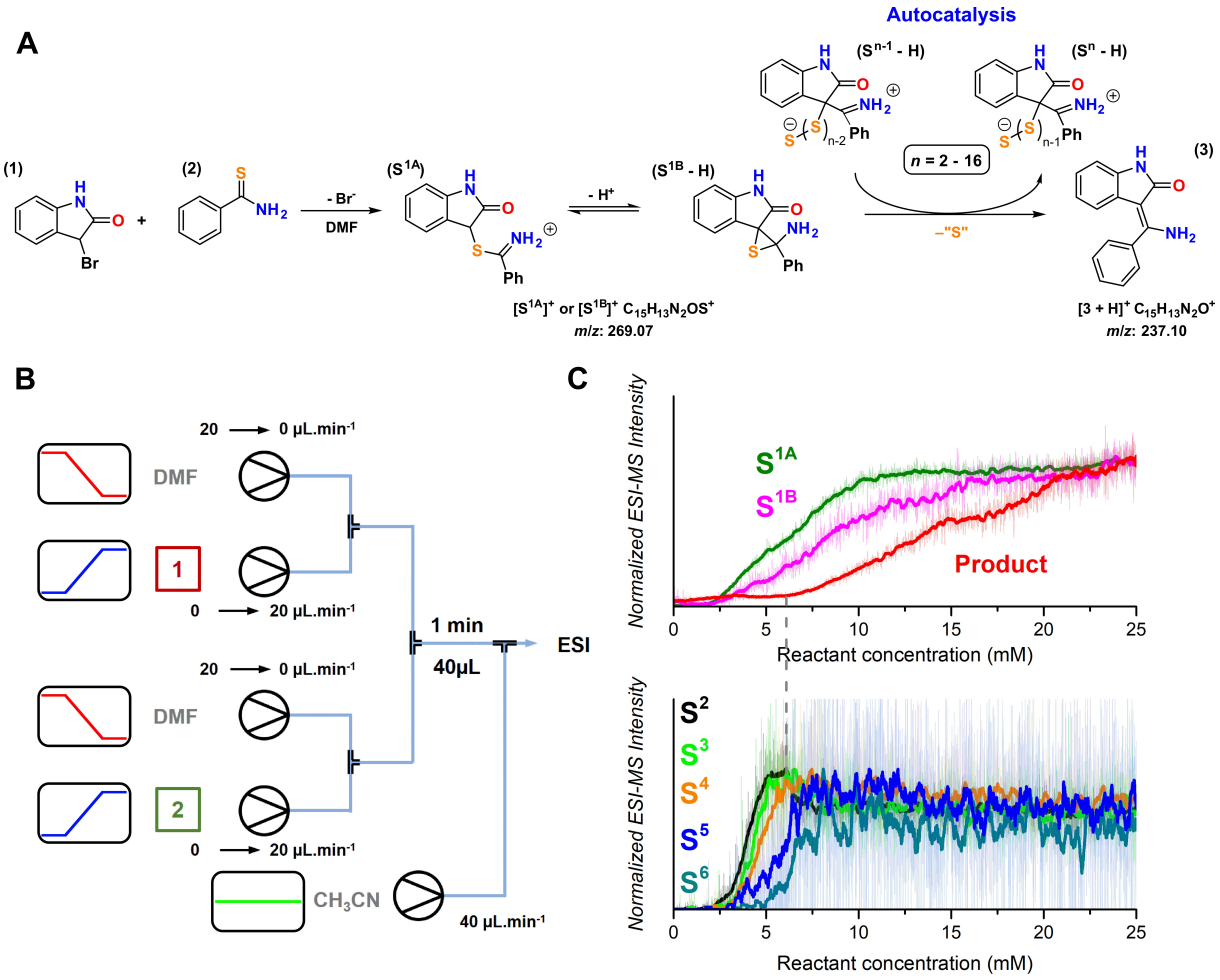

Figure 7. A. Proposed mechanism for the Eschenmoser coupling reaction based on ESI-MS measurements. B. Two syringe pumps containing reagents (1 and 2) dispensing with continuously increasing flowrates. The flowrates of two syringe pumps containing solvent (DMF) are steadily decreasing to maintain a constant reaction time in a flow reactor coupled with a mass spectrometer. C. Normalized ESI-MS intensities of reaction intermediates and product. Adapted from reference [36].

an increase in the ion intensity of targeted compound regardless of matrix effects, thus circumventing the need for absolute quantification.

Several studies harnessed flow chemistry coupled with ESI-MS to systematically screen input spaces and determine ideal reaction conditions (Figure 9A).[55,56] For instance, Browne et al. used ESI-MS to identify the best conditions for the continuous-flow preparation of benzyne, followed by its Diels-Alder cycloaddition with furan.[14] They systematically screened the impact of reaction temperature and residence time in the reactor by measuring the peak height of the desired product and determined optimum values by comparing the intensity of the product with other ions corresponding to byproducts.[14] Similarly, Haven et al. investigated polymerization reactions in commercially available microreactor chips coupled with a an ESI-MS instrument.[13] Using this setup, they systematically evaluated a range of reaction conditions including reaction temperature, residence time and reagent stoichiometry to identify ideal conditions for promoting single monomer unit insertions. This strategy enabled them to produce sequence-defined oligomers.

While the above examples systematically explored continuous experimental conditions such as concentrations or temperature, it is also possible to screen the reactivity of a range of substrates or homogeneous catalysts. In a single experiment, Martha et al. evaluated the activity of eight Lewis acids for forming imidazoline derivatives in continuous flow by injecting the catalysts into a flow reactor using an HPLC injector. The reaction plugs containing each of the catalysts yielded pulses in product ion intensity upon detection by ESI-MS.[58] The area of each pulse was directly correlated with the product concentration and thus with the catalyst activity. Similarly, the activity of various ferrocene complexes and the impact of catalyst loading was evaluated.[59]

Finally, because ESI-MS provides a real-time readout of the reaction outflow, establishing direct feedback between the MS and the flow setup enables self-optimizing experiments (Figure 9A). Rather than performing a systematic search, an algorithm adjusts the inflows to the reactor to achieve a specific

Review
doi.org/10.1002/cmtd.202400036
Chemistry Europe
European Chemical Societies Publishing

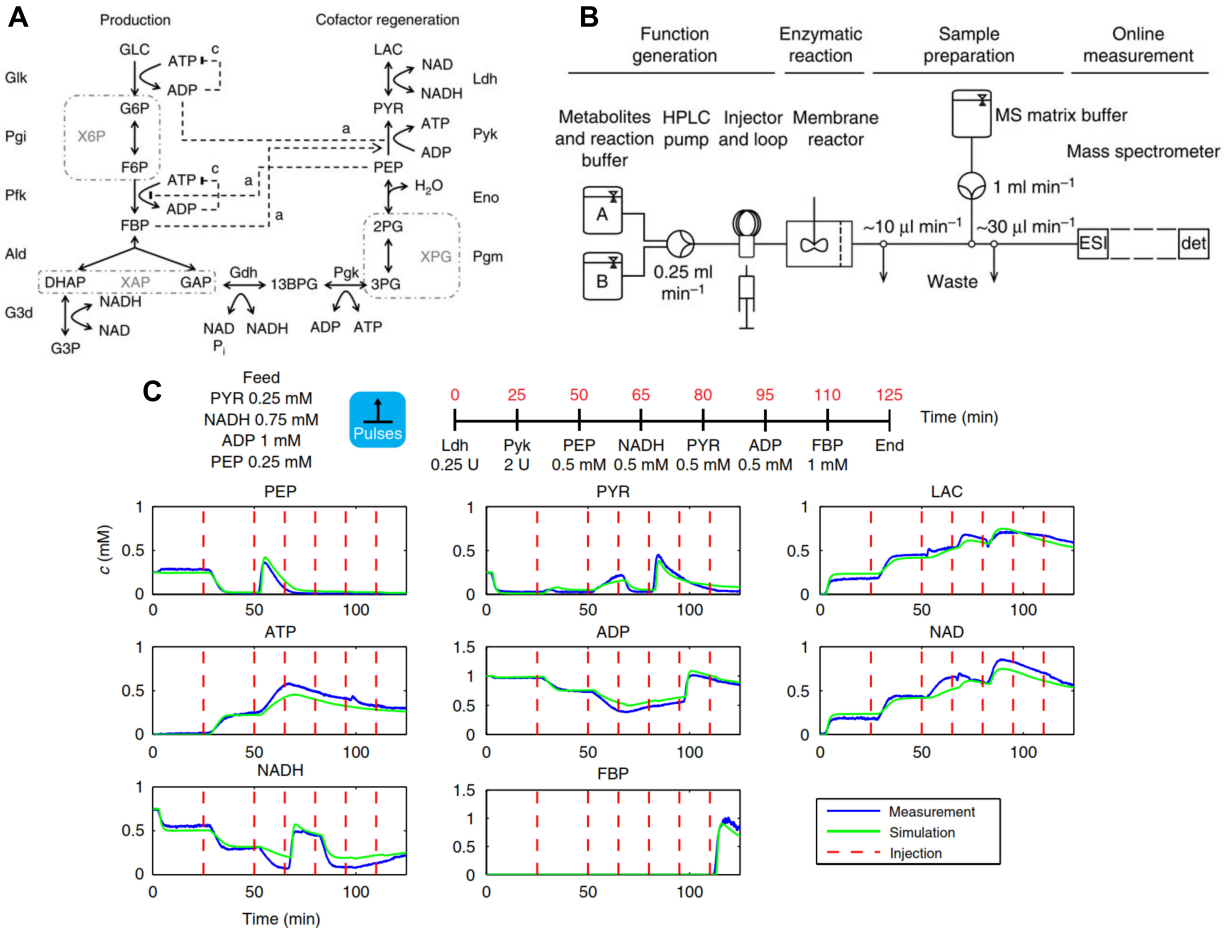

Figure 8. A. Enzymatic reaction network for the production of DHAP from glucose (GLC). B. Interface between the continuous stirred tank reactor (CSTR), in which the cascade reaction takes place, and ESI-MS. The CSTR is equipped by a membrane which retains the enzymes in the reactor while letting flow the reactants, intermediates and products. The outflow of the CSTR is diluted by a MS matrix buffer containing analytical standards used for quantification C. Pulsing perturbations of a subnetwork composed by lactase dehydrogenase (Ldh) and pyruvate kinase (Pyk). The concentration of the constant feed, along with the pulsing sequences are shown in the upper panel. The output concentrations of all metabolites measured by ESI-MS are shown in the lower panels. Adapted from reference [51].

goal, *i.e.*, obtaining the maximum ion intensity for a desired product while minimizing the abundance of byproducts or consumption of certain reagents. The algorithm thus autonomously performs the search through the input space without the need for human intervention. For instance, Holmes and colleagues reported the self-optimization of methyl nicotinate amidation.[57] This substrate was specifically chosen due to the presence of the pyridine moiety, which readily ionizes by protonation. Moreover, the amide product can hydrolyse to yield the corresponding carboxylic acid, thereby resulting in a loss of selectivity.

The two reagents, methyl nicotinate and methylamine (Figure 9C), along with solvent, are continuously pumped in a tubular reactor with active heating and cooling. The reactor outflow was sampled with a 4-port sample loop and diluted before infusion into the MS (Figure 9B). The ESI-MS data were continuously read and the product yield was calculated based on a calibration curve. Upon reaching a steady state for given initial conditions, the reaction temperature and inflows of ester and methylamine were adjusted by an algorithm to reach a new set of conditions. As shown in Figure 9C, the optimum yield of N′-methyl nicotinamide was reached in 21 iterations corresponding to 12 h of experimental time.[57] A experimental design approach was also followed and led to nearly identical optimum conditions.

Similarly, Fitzpatrick et al. reported the self-optimization of the heterogeneous hydration of a nitrile over a packed bed of MnO_2.[60] In their setup, the reaction temperature, residence time and nitrile concentration were autonomously optimized by maximizing the ratio between the ion intensities of the product and substrate ions. Using an in-house algorithm, the objective was achieved within 12 iterations carried out over 17 h of experimental time. Finally, integrating inline FT-IR spectroscopy and online MS was also reported for the optimization of an organometallic C–C coupling mediated by n-butyllithum.[61] In this case, the product and starting materials were quantified by FT-IR measurements while MS was used to detect byproduct formation. The reaction temperature, residence time and stoichiometric ratios between reagents were autonomously

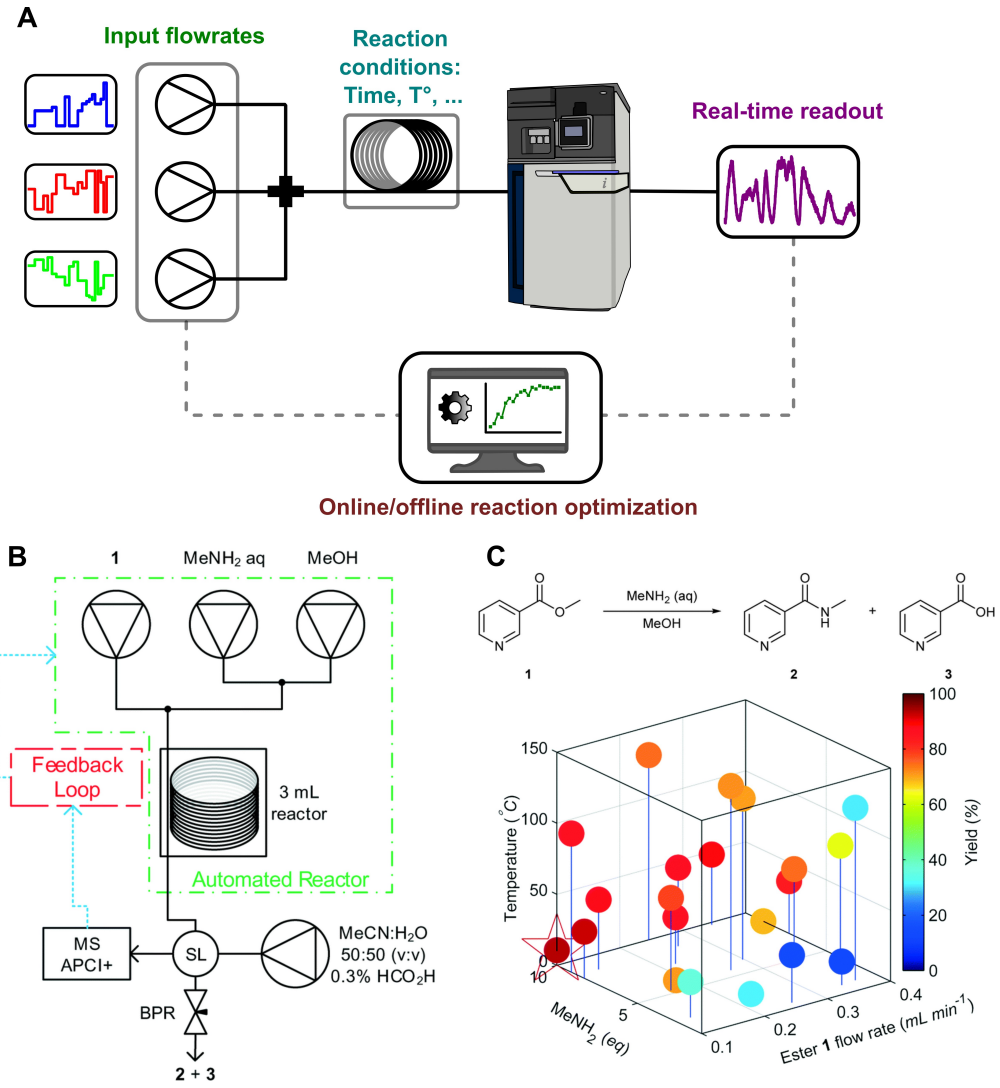

Figure 9. A. Representation of a feedback between the continuous flow chemistry setup and the ESI-MS readout for reaction optimization. The optimization can be carried out offline by systematically screening the input space and selecting the best reaction conditions, or online by autonomously adjusting the reaction parameters to reach a specific goal. B. Example of reactor setup as reported by Holmes et al. Reagents are pumped in a tubular reactor sampled by a 4-port sample loop (SL). The outflow is diluted by solvent prior to infusion in the MS instrument, and the whole setup is maintained under pressure using a back pressure regulator (BPR). C. Top: Amidation of methyl nicotinate (1) leading to N′-methyl nicotinamide (2) and impurity niacin (3). Bottom: Results of the self-optimization experiment, where the reaction temperature and flowrates of methyl nicotinate and methylamine are varied. The optimal conditions are highlighted by a star. Adapted with permission from reference [57].

optimized to reach maximum product yield while minimizing byproduct formation.

Although only a handful implementations have been reported for optimization or self-optimization, the interface between flow chemistry and ESI-MS holds promise for dealing with a wider range of reactions including photocatalysis or electrocatalysis. Leveraging autonomous MS approaches has the potential to streamline the screening and development of complex synthetic pathways while significantly reducing experimental time and efforts.

Summary and Outlook

Continuous flow chemistry stands out as transformative synthetic method that facilitates the exploration of input spaces and enables process automation, while improving reproducibility, scalability, and overall safety. In this context of high-throughput exploration of chemical reactivity, the analysis of reaction mixtures can become an obstacle. Integrating flow chemistry with ESI-MS is particularly effective as it allows for the individual observation of many compounds from a reaction medium, including low abundance species. When coupled to add-on methods, ESI-MS provides structural information beyond simple mass detection.[29,31,33] Moreover, the sensitivity and time resolution of MS approaches enable to map how a reaction adapts to changing conditions.[51,53] This allows for (*i*)

gathering mechanistic insights by monitoring the formation and reactivity of intermediates in solution or in the gas phase[21,30,36,44,47] or (*ii*) extensive screening through large input spaces to determine ideal reaction conditions.[13,14,57,60] It is worth noting that other approaches have been developed for reaction monitoring with mass spectrometry, such as the coupling ofdroplet microfluidics with ESI-MS,[62,63] or the analysis of high-throughput experimentation conducted in bulk microtiter plates by desorption electrospray ionization mass spectrometry (DESI-MS).[64,65] However, those approaches do not allow to probe reaction dynamics in real time, or to easily probe the impact of reaction times. Moreover, they cannot be easily integrated with automated approaches enabling the self-optimization of reaction conditions.

Reaction monitoring via flow chemistry coupled with MS has limitations. First, the processes associated with ESI may lead to reaction acceleration[66] or to the formation of artifacts[42] that are not relevant for solution chemistry. Moreover, reactions leading to precipitates cannot be investigated as they might clog the source inlet. Sampling is also a crucial parameter as the ESI source can become contaminated after prolonged exposure to concentrated reaction mixtures, though this can be mitigated using dilution lines or sample loops.[57] Finally, as briefly discussed in the introduction, because of matrix effects associated with the analysis of crude reaction mixtures, the ESI-MS response does not always correlate with changes in solution concentration.[12] Care must thus be taken when interpreting solution-phase processes based on MS data, even though quantitative approaches relying of isotopically labelled compounds have been reported.[25,50,51,53]

Nonetheless, its sensitivity and ability to detect many components simultaneously make ESI-MS a unique player for online reaction monitoring. Combined with the versatility and modularity of flow chemistry, it is hoped that the integration of both approaches will open new doors for the exploration of photochemical, electrochemical, or cascade reactions. Moreover, the development of self-driving reaction optimization platforms integrating flow reactors and mass spectrometry[57,60,61] will be instrumental in streamlining the development of complex synthetic pathways and, looking forward, will certainly contribute to uncover novel types of chemistry.

Acknowledgments

This work has been funded by a FRS-FNRS postdoctoral fellowship. I would like to thank Prof. Pascal Gerbaux, Dr. Julien De Winter and Dr. Mònica Rodríguez Serrat for proof-reading this manuscript and for their continuous support. I also thank Prof. Jana Roithová and Prof. Wilhelm Huck for their guidance and support.

Conflict of Interests

The author declares no competing financial interest.

Data Availability Statement

Data sharing is not applicable to this article as no new data were created or analyzed in this study.

Keywords: Mass spectrometry · Flow chemistry · Reaction mechanisms · Reaction intermediates · High-throughput screening

[1] L. Capaldo, Z. Wen, T. Noel, *Chem. Sci.* **2023**, *14*, 4230–4247.
[2] M. G. Russell, T. F. Jamison, *Angew. Chem. Int. Ed.* **2019**, *58*, 7678–7681.
[3] S. B. Otvos, M. A. Pericas, C. O. Kappe, *Chem. Sci.* **2019**, *10*, 11141–11146.
[4] L. Buglioni, F. Raymenants, A. Slattery, S. D. A. Zondag, T. Noel, *Chem. Rev.* **2022**, *122*, 2752–2906.
[5] T. S. Chen, H. Long, Y. Gao, H. C. Xu, *Angew. Chem. Int. Ed.* **2023**, *62*, e202310138.
[6] S. Steiner, J. Wolf, S. Glatzel, A. Andreou, J. M. Granda, G. Keenan, T. Hinkley, G. Aragon-Camarasa, P. J. Kitson, D. Angelone, L. Cronin, *Science* **2019**, *363*, eaav221.
[7] A. A. Volk, R. W. Epps, D. T. Yonemoto, B. S. Masters, F. N. Castellano, K. G. Reyes, M. Abolhasani, *Nat. Commun.* **2023**, *14*, 1403.
[8] A. Slattery, Z. Wen, P. Tenblad, J. Sanjose-Orduna, D. Pintossi, T. den Hartog, T. Noel, *Science* **2024**, *383*, eadj1817.
[9] M. Rodriguez-Zubiri, F.-X. Felpin, *Org. Proc. Res. Dev.* **2022**, *26*, 1766–1793.
[10] L. P. Yunker, R. L. Stoddard, J. S. McIndoe, *J. Mass Spectrom.* **2014**, *49*, 1–8.
[11] K. L. Vikse, Z. Ahmadi, C. C. Manning, D. A. Harrington, J. S. McIndoe, *Angew Chem Int Ed Engl* **2011**, *50*, 8304–8306.
[12] J. Mehara, J. Roithová, *Chem. Sci.* **2020**, *11*, 11960–11972.
[13] J. J. Haven, J. Vandenbergh, T. Junkers, *Chem. Commun.* **2015**, *51*, 4611–4614.
[14] D. L. Browne, S. Wright, B. J. Deadman, S. Dunnage, I. R. Baxendale, R. M. Turner, S. V. Ley, *Rapid Commun. Mass Spectrom.* **2012**, *26*, 1999–2010.
[15] J. S. Mathieson, M. H. Rosnes, V. Sans, P. J. Kitson, L. Cronin, *Beilstein J. Nanotechnol.* **2013**, *4*, 285–291.
[16] Z. Wei, Y. Li, R. G. Cooks, X. Yan, *Annu. Rev. Phys. Chem.* **2020**, *71*, 31–51.
[17] D. L. Stares, A. Szumna, C. A. Schalley, *Chem. Eur. J.* **2023**, *29*, e202302112.
[18] K. L. Vikse, J. S. McIndoe, *Pure Appl. Chem.* **2015**, *87*, 361–377.
[19] L. P. E. Yunker, Z. Ahmadi, J. R. Logan, W. Wu, T. Li, A. Martindale, A. G. Oliver, J. S. McIndoe, *Organometallics* **2018**, *37*, 4297–4308.
[20] P. J. H. Williams, C. Killeen, I. C. Chagunda, B. Henderson, S. Donnecke, W. Munro, J. Sidhu, D. Kraft, D. A. Harrington, J. S. McIndoe, *Chem. Sci.* **2023**, *14*, 9970–9977.
[21] L. S. Santos, J. O. Metzger, *Angew. Chem. Int. Ed.* **2006**, *45*, 977–981.
[22] V. Gabelica, E. Marklund, *Curr. Opin. Chem. Biol.* **2018**, *42*, 51–59.
[23] L. Polewski, A. Springer, K. Pagel, C. A. Schalley, *Acc Chem Res* **2021**, *54*, 2445–2456.
[24] N. Geue, T. S. Bennett, A. A. Arama, L. A. I. Ramakers, G. F. S. Whitehead, G. A. Timco, P. B. Armentrout, E. J. L. McInnes, N. A. Burton, R. E. P. Winpenny, P. E. Barran, *J. Am. Chem. Soc.* **2022**, *144*, 22528–22539.
[25] Q. Duez, P. Tinnemans, J. A. A. W. Elemans, J. Roithová, *Chem. Sci.* **2023**, *14*, 9759–9769.
[26] P. Thordarson, E. J. A. Bijsterveld, A. E. Rowan, R. J. M. Nolte, *Nature* **2003**, *424*, 915–918.
[27] J. A. A. W. Elemans, R. J. M. Nolte, *Chem. Comm.* **2019**, *55*, 9590–9605.
[28] J. A. A. W. Elemans, E. J. A. Bijsterveld, A. E. Rowan, R. J. M. Nolte, *Eur. J. Org. Chem.* **2007**, *2007*, 751–757.
[29] X. Chen, Q. Duez, G. L. Tripodi, P. J. Gilissen, D. Piperoudis, P. Tinnemans, J. A. A. W. Elemans, J. Roithová, R. J. M. Nolte, *Eur. J. Org. Chem.* **2022**, *2022*, e202200280.
[30] M. Rodríguez, A. Y. Pereverzev, J. Roithová, *ChemCatChem* **2023**, *15*, e202300410.
[31] G. L. Tripodi, M. M. J. Dekker, J. Roithová, L. Que, Jr., *Angew. Chem. Int. Ed.* **2021**, *60*, 7126–7131.
[32] J. Roithová, A. Gray, E. Andris, J. Jašík, D. Gerlich, *Acc. Chem. Res.* **2016**, *49*, 223–230.
[33] M. Pahl, M. Mayer, M. Schneider, D. Belder, K. R. Asmis, *Anal. Chem.* **2019**, *91*, 3199–3203.

[34] M. Mayer, M. Pahl, M. Spanka, M. Grellmann, M. Sickert, C. Schneider, K. R. Asmis, D. Belder, *Phys. Chem. Chem. Phys.* **2020**, *22*, 4610–4616.
[35] S. Schmahl, F. Horn, J. Jin, H. Westphal, D. Belder, K. R. Asmis, *ChemPhysChem* **2024**, *25*, e202300975.
[36] Q. Duez, L. Marek, J. Vana, J. Hanusek, J. Roithová, *Chem. Eur. J.* **2024**, *30*, e202303619.
[37] Y. Lee, G. L. Tripodi, D. Jeong, S. Lee, J. Roithová, J. Cho, *J. Am. Chem. Soc.* **2022**, *144*, 20752–20762.
[38] R. Bakker, A. Bairagi, M. Rodriguez, G. L. Tripodi, A. Y. Pereverzev, J. Roithová, *Inorg. Chem.* **2023**, *62*, 1728–1734.
[39] J. Luo, A. G. Oliver, J. S. McIndoe, *Dalton Trans* **2013**, *42*, 11312–11318.
[40] A. J. Ingram, K. L. Walker, R. N. Zare, R. M. Waymouth, *J. Am. Chem. Soc.* **2015**, *137*, 13632–13646.
[41] L. Konermann, F. I. Rosell, A. G. Mauk, D. J. Douglas, *Biochemistry* **1997**, *36*, 6448–6454.
[42] W. Jiang, A. Schäfer, P. C. Mohr, C. A. Schalley, *J. Am. Chem. Soc.* **2010**, *132*, 2309–2320.
[43] L. Konermann, B. A. Collings, D. J. Douglas, *Biochemistry* **1997**, *36*, 5554–5559.
[44] G. L. Tripodi, M. T. G. M. Derks, F. P. J. T. Rutjes, J. Roithová, *Chemistry-Methods* **2021**, *1*, 430–437.
[45] D. J. Wilson, L. Konermann, *Anal. Chem.* **2003**, *75*, 6408–6414.
[46] D. J. Wilson, L. Konermann, *Anal. Chem.* **2004**, *76*, 2537–2543.
[47] E. J. Meeus, M. T. G. M. Derks, N. P. van Leest, C. J. Verhoef, J. Roithová, J. N. H. Reek, B. de Bruin, *Chem Catalysis* **2023**, *3*, 100700.
[48] J. Yang, G. L. Tripodi, M. Derks, M. S. Seo, Y. M. Lee, K. W. Southwell, J. Shearer, J. Roithová, W. Nam, *J. Am. Chem. Soc.* **2023**, *145*, 26106–26121.
[49] M. G. Baltussen, T. J. de Jong, Q. Duez, W. E. Robinson, W. T. S. Huck, *Nature* **2024**, *631*, 549–555.
[50] M. Bujara, M. Schumperli, R. Pellaux, M. Heinemann, S. Panke, *Nat. Chem. Biol.* **2011**, *7*, 271–277.
[51] C. Hold, S. Billerbeck, S. Panke, *Nat. Commun.* **2016**, *7*, 12971.
[52] M. G. Baltussen, J. van de Wiel, C. L. Fernandez Regueiro, M. Jakstaite, W. T. S. Huck, *Anal. Chem.* **2022**, *94*, 7311–7318.
[53] Q. Duez, J. van de Wiel, B. van Sluijs, S. Ghosh, M. G. Baltussen, M. T. G. M. Derks, J. Roithová, W. T. S. Huck, *J. Am. Chem. Soc.* **2024**, *146*, 20778–20787.
[54] B. van Sluijs, T. Zhou, B. Helwig, M. G. Baltussen, F. H. T. Nelissen, H. A. Heus, W. T. S. Huck, *Nat. Commun.* **2024**, *15*, 1602.
[55] B. P. Loren, M. Wleklinski, A. Koswara, K. Yammine, Y. Hu, Z. K. Nagy, D. H. Thompson, R. G. Cooks, *Chem. Sci.* **2017**, *8*, 4363–4370.
[56] D. Hadavi, P. Han, M. Honing, *J. Flow. Chem.* **2021**, *12*, 175–184.
[57] N. Holmes, G. R. Akien, R. J. D. Savage, C. Stanetty, I. R. Baxendale, A. J. Blacker, B. A. Taylor, R. L. Woodward, R. E. Meadows, R. A. Bourne, *React. Chem. Eng.* **2016**, *1*, 96–100.
[58] C. T. Martha, N. Elders, J. G. Krabbe, J. Kool, W. M. A. Niessen, R. V. A. Orru, H. Irth, *Anal. Chem.* **2008**, *80*, 7121–7127.
[59] C. T. Martha, A. Heemskerk, J. C. Hoogendoorn, N. Elders, W. M. Niessen, R. V. Orru, H. Irth, *Chem. Eur. J.* **2009**, *15*, 7368–7375.
[60] D. E. Fitzpatrick, C. Battilocchio, S. V. Ley, *Org. Proc. Res. Dev.* **2015**, *20*, 386–394.
[61] V. Fath, P. Lau, C. Greve, P. Weller, N. Kockmann, T. Röder, *J. Flow. Chem.* **2021**, *11*, 285–302.
[62] E. E. Kempa, C. A. Smith, X. Li, B. Bellina, K. Richardson, S. Pringle, J. L. Galman, N. J. Turner, P. E. Barran, *Anal. Chem.* **2020**, *92*, 12605–12612.
[63] K. Wink, M. van der Loh, N. Hartner, M. Polack, C. Dusny, A. Schmid, D. Belder, *Angew. Chem. Int. Ed.* **2022**, *61*, e202204098.
[64] B. P. Loren, H. S. Ewan, L. Avramova, C. R. Ferreira, T. J. P. Sobreira, K. Yammine, H. Liao, R. G. Cooks, D. H. Thompson, *Sci. Rep.* **2019**, *9*, 14745.
[65] Z. Jaman, D. L. Logsdon, B. Szilagyi, T. J. P. Sobreira, D. Aremu, L. Avramova, R. G. Cooks, D. H. Thompson, *ACS Comb. Sci.* **2020**, *22*, 184–196.
[66] K. H. Huang, Z. Wei, R. G. Cooks, *Chem. Sci.* **2020**, *12*, 2242–2250.

Manuscript received: August 30, 2024
Version of record online: ■■, ■■